

Analytical modelling of air-cored partially HTS motor with permanent magnet rotor

Zhishu Qiu

Department of Electronic and Electrical
Engineering
University of Strathclyde
Glasgow, UK
zhishu.qiu.2018@uni.strath.ac.uk

Min Zhang

Department of Electronic and Electrical
Engineering
University of Strathclyde
Glasgow, UK
min.zhang@uni.strath.ac.uk

Alexandre Colle

Airbus UpNext
Airbus ExO Zero Emissions
Blagnac, France
alexandre.colle@airbus.com

Abstract— An analytical technique for finding machine equivalent circuit variables of air-cored radial flux partially HTS motor is developed. This synchronous motor has HTS armature windings and permanent magnet rotor. It is achieved through MATLAB coding, and the output variables include induced electromotive force (EMF), HTS armature winding inductance and its equivalent ac resistance. The output from this 2-d analytical modelling is compared with the results from corresponding finite element modelling.

Keywords— analytical modelling, synchronous motor, HTS winding

I. INTRODUCTION

This study introduces general analytical modelling for air-cored radial flux PM-HTS (i.e. permanent magnet rotor and HTS stator) motor. The analytical modelling will be realized through simplified MATLAB coding. The expected model output as shown in Fig.1 aims to obtain machine equivalent circuit variables for a given voltage and rated power. The modelling process is given as follows. The induced electromotive force (EMF) will be calculated through rotor magnetic field analysis, armature winding inductance will be determined by armature reaction field, and ac loss of armature winding will help figure out equivalent ac resistance. All the results obtained will be checked through numerical modelling. Although this study only considers the steady state mode, transient fault conditions such as short circuits are worth analysing in the future.

II. STRUCTURE OF THE MACHINE

A schematic cross-sectional view of the air-cored radial flux PM-HTS motor is given in Fig.2, where R_r is the rotor hub radius, R_g represents the mean air gap radius and R_s is the outer radius of the stator winding. As curve length is close to straight-line length when it is small, it is reasonable to simplify sector shape cross-section to a rectangular shape in the magnetic field study. The rotor magnet is mounted on the surface of the rotor yoke, and the distributed HTS winding is chosen for the stator.

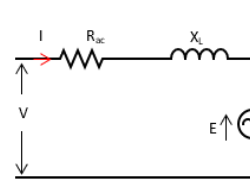


Fig. 1. Machine equivalent circuit diagram

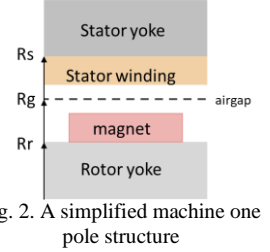


Fig. 2. A simplified machine one pole structure

III. MODELLING METHODOLOGY

A. Magnetic Field Distribution

The induced EMF depends on the rotor magnetic field. Hence the main task here is to model airgap flux density. A 2-d analytical method for predicting open-circuit field distribution is proposed analysis in [1]. The method considers n th harmonic component, in general, for inner rotor topology, no-load rotor magnetic field distribution in both radial and axial directions respectively are given in (1) and (2) at the end of the paper and residual magnetization vector,

$$M_n = 2(B_r/\mu_0)\sin[(n\pi\alpha_p)/2]/[(n\pi\alpha_p)/2] \quad (3)$$

Where p is the pole pair number, R_m is the magnet surface radius, residual magnetization vector M_n , and α_p is the magnet pole-arc to pole-pitch ratio. Harmonic components considered in this study are fundamental, 3rd, 5th, 7th and 9th. This model is validated through numerical modelling in COMSOL. A case study of radial flux density distribution as illustrated in Fig. 3 shows good consistency.

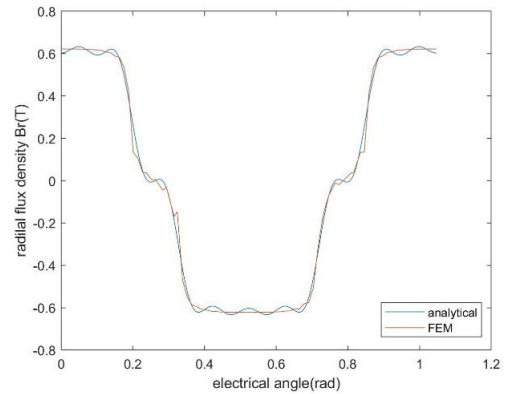


Fig. 3. Analytical modelling validation of rotor radial flux density

B. Inductance of Armature Winding

The inductance is obtained through the definition of induced emf:

$$\text{emf} = N(d\phi/dt) = L(di/dt) \quad (4)$$

Where N is the winding turn per phase and L is the self-inductance per phase. Considering mutual inductance between phases, paper [2] proposed a factor, k_L that can transfer inductance per phase to total three phase inductance

$$k_L = 4(\pi - \kappa)/(3\pi - 4\kappa) \quad (5)$$

Where κ is the half angular width of a winding slot. The results of analytical modelling are compared with results obtained from finite element modelling (FEM). The method used in FEM is to calculate inductance through magnetic energy,

$$E_{p,m} = LI^2/2 \quad (6)$$

As can be seen in the case study results, analytical modelling agrees well with FEM, only gives about 1% difference lower than the FEM value.

TABLE I. INDUCTANCE MODELLING CASE STUDY RESULTS

Inductance	Analytical	FEM	Unit
1 phase	49.5	50.08	uH
3 phase	66.9	-	uH

C. AC Resistance of Armature Winding

AC resistance of HTS tape is determined by working temperature, frequency and the machine geometry. It is hard to describe it through one equation, therefore, in this study ac resistance is calculated through the definition of ac losses,

$$P_{\text{loss}} = I^2 R_{\text{ac}} \quad (7)$$

where ac losses of HTS tapes are obtained through numerical modelling in COMSOL using T-A formulation[3]. T-A formula approach solves two state variables separately. The current vector potential, \mathbf{T} along with the HTS tapes layer, and the magnetic vector potential, \mathbf{A} for the whole geometry. The governing equations are given:

$$\mathbf{J} = \nabla \times \mathbf{T} \quad (8)$$

$$\nabla \times \rho \nabla \times \mathbf{T} = -\partial \mathbf{B} / \partial t \quad (9)$$

Where μ is the magnetic permeability, \mathbf{J} is the current density and ρ is the resistivity.

An ac resistance worked example of a 12 poles machine is given here, only one-twelfth of the machine (i.e. one pole) is modelled for calculation time efficiency reason. Fig. 4 gives one-twelfth machine model in detail in COMSOL, and

the simulation work regarding to different working temperatures as well as electrical loadings has been completed. The working temperature range is between 30 K to 75K. The rated current is assumed to be 1000 A, and the electrical loading varies from 10% to 100% of rated loading. The final ac resistance values are plotted in Fig. 5, the curves are reasonable since ac loss is proportional to the square of current I .

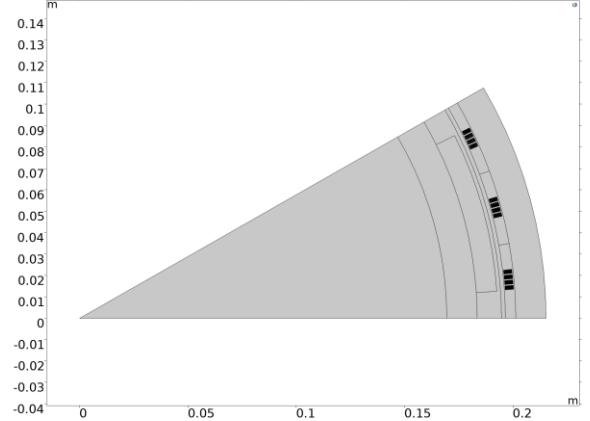


Fig. 4. One pole of machine model built in COMSOL

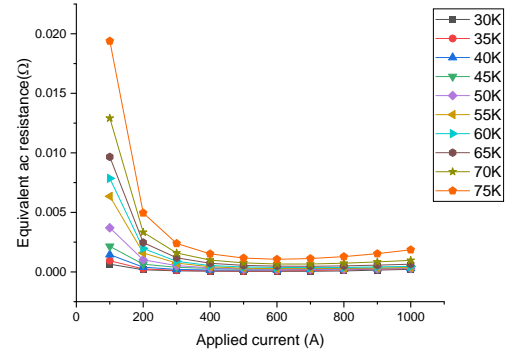


Fig. 5. Example results of equivalent ac resistance

REFERENCES

- [1] Z. Q. Zhu and D. Howe, "Instantaneous magnetic field distribution in brushless permanent magnet DC motors. III. Effect of stator slotting," *IEEE Transactions on Magnetics*, vol. 29, no. 1, pp. 143-151, 1993, doi: 10.1109/20.195559.
- [2] J. Engström, "Inductance of Slotless Machines," *IEEE Nordic Workshop on Power and Industrial Electronics*, 2000.
- [3] H. Zhang, M. Zhang, and W. Yuan, "An efficient 3D finite element method model based on the T-A formulation for superconducting coated conductors," *Superconductor Science and Technology*, vol. 30, no. 2, p. 024005, 2016/12/13 2016, doi: 10.1088/1361-6668/30/2/024005.

$$B_r(r, \theta) = \sum_{n=1,3,5,\dots}^{\infty} \frac{\mu_0 M_n}{\mu_r} \frac{np}{(np)^2 - 1} \cdot \left\{ \frac{(np-1) + 2\left(\frac{R_r}{R_m}\right)^{np+1} - (np+1)\left(\frac{R_r}{R_m}\right)^{2np}}{\mu_r + 1 \left[1 - \left(\frac{R_r}{R_s}\right)^{2np}\right] - \frac{\mu_r - 1}{\mu_r} \left[\left(\frac{R_m}{R_s}\right)^{2np} - \left(\frac{R_r}{R_m}\right)^{2np}\right]} \right\} \cdot \left[\left(\frac{r}{R_s}\right)^{np-1} \left(\frac{R_m}{R_s}\right)^{np+1} + \left(\frac{R_m}{r}\right)^{np+1} \right] \cos np\theta \quad (1)$$

$$B_\theta(r, \theta) = \sum_{n=1,3,5,\dots}^{\infty} \frac{-\mu_0 M_n}{\mu_r} \frac{np}{(np)^2 - 1} \cdot \left\{ \frac{(np-1) + 2\left(\frac{R_r}{R_m}\right)^{np+1} - (np+1)\left(\frac{R_r}{R_m}\right)^{2np}}{\mu_r + 1 \left[1 - \left(\frac{R_r}{R_s}\right)^{2np}\right] - \frac{\mu_r - 1}{\mu_r} \left[\left(\frac{R_m}{R_s}\right)^{2np} - \left(\frac{R_r}{R_m}\right)^{2np}\right]} \right\} \cdot \left[\left(\frac{r}{R_s}\right)^{np-1} \left(\frac{R_m}{R_s}\right)^{np+1} - \left(\frac{R_m}{r}\right)^{np+1} \right] \sin np\theta \quad (2)$$